Title

Lipid metabolism disorder induced by up-regulation of miR-125b and miR-144 following β-diketone antibiotic exposure to F0-zebrafish (Danio rerio)

Authors

Wang, Xuedong
Zheng, Yuansi
Ma, Yan
et al.

Publication Date

2018-11-01

DOI

10.1016/j.ecoenv.2018.08.027

Peer reviewed

Ecotoxicology and Environmental Safety 164 (2018) 243–252

Contents lists available at ScienceDirect

Ecotoxicology and Environmental Safety

journal homepage: www.elsevier.com/locate/ecoenv

Lipid metabolism disorder induced by up-regulation of miR-125b and miR-144 following β-diketone antibiotic exposure to F0-zebrafish (*Danio rerio*)

Xuedong Wang[a], Yuansi Zheng[b], Yan Ma[c], Liyang Du[a], Fangyu Chu[a], Haidong Gu[a], Randy A. Dahlgren[d], Yanyan Li[c,*], Huili Wang[a,*]

[a] Jiangsu Key Laboratory of Environmental Science and Engineering, School of Environmental Science and Engineering, Suzhou University of Science and Technology, Suzhou 215009, China
[b] Department of Pathology, Zhejiang Cancer Hospital, Hangzhou 310022, China
[c] College of Life Sciences, Wenzhou Medical University, Wenzhou 325035, China
[d] Department of Land, Air and Water Resources, University of California, Davis, CA 95616, USA

ARTICLE INFO

Keywords:
β-Diketone antibiotics (DKAs)
Zebrafish
MiRNA
Gene therapy
Lipid metabolism
Toxicology

ABSTRACT

β-Diketone antibiotics (DKAs) are widely used in human and veterinary medicine to prevent and treat a large variety of infectious diseases. Long-term DKA exposure to zebrafish can result in lipid metabolism disorders and liver function abnormalities. Based on our previous miRNA-seq analyses, miR-144 and miR-125b were identified as target genes regulating lipid metabolism. DKA-exposure at 12.5 and 25 mg/L significantly increased the expressions of miR-144 and miR-125b. The expression levels for the two miRNAs exhibited an inverse relationship with their lipid-metabolism-related target genes (*ppardb*, *bcl*2a, *pparaa* and *pparda*). Over-expression and inhibition of miR-144 and miR-125b were observed by micro-injection of *agomir-144*, *agomir-125b*, *antagomir-144* and *antagomir-125b*. The over-expression of miR-144 and miR-125b enhanced lipid accumulation and further induced lipid-metabolism-disorder syndrome in F1-zebrafish. The expression of *ppardb* and *bcl2a* in whole-mount *in situ* hybridization was in general agreement with results from qRT-PCR and was concentration-dependent. Oil red O and H&E staining, as well as related physiological and biochemical indexes, showed that chronic DKA exposure resulted in lipid-metabolism-disorder in F0-adults, and in F1-larvae fat accumulation, increased lipid content, abnormal liver function and obesity. The abnormal levels of triglyceride (TG) and total cholesterol (TCH) in DKA-exposed zebrafish increased the risk of hyperlipidemia, atherosclerosis and coronary heart disease. These observations improve our understanding of mechanisms leading to liver disease from exposure to environmental pollution, thereby having relevant practical significance in health prevention, early intervention, and gene therapy for drug-induced diseases.

1. Introduction

MicroRNAs, abbreviated as miRNAs or miRs, are small non-coding regulatory RNAs that post-transcriptionally regulate gene expression by inducing cleavage of their target mRNAs or by inhibiting their translation or causing degradation of the target messenger RNAs (Krol et al., 2010). MiRNAs are identified as key regulators in governing physiological and pathological processes. Some circulating miRNAs are found in body fluids including saliva, urine and blood (Weber et al., 2010). Chen et al. (2008) found that circulating miRNAs hold considerable potential as biomarkers for several diseases, including Type 2 diabetes (T2D), insulin resistance and metabolic syndrome. Several miRNAs, such as miR-122, miR-33, miR-24 and miR130a-3p, have been implicated in controlling both insulin signaling and glucose metabolism at multiple levels (Ng et al., 2014; Xiao et al., 2014). miRNA-144 is a key miRNA in the pathological process of T2D, which is an important component of the insulin-signaling cascade that plays an important role in regulating insulin in muscles (Karolina et al., 2011). Enhanced expression of miR-144 can be considered as a biomarker for medullary thyroid carcinoma (MTC), providing significant predictive value for patients with MTC (Shabani et al., 2018). In particular, miR-144-3p is down-regulated in various cancers, and its overexpression inhibits the proliferation and metastasis of cancer cells (Song et al., 2018). Further, one study indicated that LncRNA TUG1 interacts with miR-144 contributing to proliferation, migration and tumorigenesis through activation of the JAK2/STAT3 pathway in hepatocellular carcinoma (Lv et al., 2018). In

* Corresponding authors.
E-mail addresses: liyan@wzmc.edu.cn (Y. Li), wxdong@wzmc.edu.cn (H. Wang).

https://doi.org/10.1016/j.ecoenv.2018.08.027
Received 24 January 2018; Received in revised form 5 August 2018; Accepted 7 August 2018

summary, the regulatory functions of miR-144 are mainly concerned with cancer cell proliferation and migration, stem cell differentiation, inflammation, apoptosis and erythroid differentiation.

In contrast to miR-144, there is a paucity of data regarding the regulatory functions of miR-125b. Li et al. (2018) reported that a miR-125 inhibitor restored the proliferation and migration potentials of cardiac progenitor cells after MALAT1 knockdown by hypoxia. The aberrant expression of the miR-125 family is strongly related to tumorigenesis and tumor development through regulation of downstream targets, including transcription factors like STAT3, cytokines like IL-6 and TGF-β, tumor suppressing protein p53, pro-apoptotic protein Bak1 and RNA binding protein. Nowadays, miR-125b has become a putative and valuable biomarker for cancer diagnosis, treatment and prognosis (Yin et al., 2015). miR-125-5p levels decreased dramatically in atypia of hepatocytes, and miR-125b played a key role in innate immune response (Xu et al., 2018). Lipopolysaccharide (LPS) stimulation of mice Raw 264.7 macrophages resulted in down-regulation of miR-125b levels, similar to the changes observed when C57BL/6 mice were i.p. injected with LPS (Tili et al., 2007). In spite of this previous research, the regulatory effects of miR-144 and miR-125b on zebrafish fat metabolism and related mechanisms have not been rigorously studied and remain uncertain.

β-Diketone antibiotics (DKAs), including fluoroquinolones (FQs) and tetracyclines (TCs), are an important antibiotic class commonly used in pharmaceuticals and personal care products. They are widely used in human and veterinary medicine to prevent and treat a large variety of infectious diseases (Alavi et al., 2015). Long-term use of DKAs can result in immune toxicity, feminization, reproductive failure, abortion, *etc.* (Mulgaonkar et al., 2012). Our group previously investigated the effects of FQs, TCs and their mixtures on zebrafish growth, development and behavior, and found that FQs and TCs had synergistic effects (Zhang et al., 2018). The body mass index (BMI) and viscera index (VI) were significantly increased upon 25 mg/L DKA exposure to zebrafish from 4-hpf to 90 dpf (Li et al., 2016). After a 3-month DKA exposure to F0-zebrafish, 11 miRNAs with significant differential expression and high-abundance were identified by means of high throughput sequencing in F1-zebrafish, among which miR-144 and miR-125b were two prominent up-regulated candidate miRNAs. With the prevalence of obesity and metabolic syndrome, non-alcoholic fatty liver disease (NAFLD) has become the most common chronic liver disease worldwide. Based on the “multiple hit” theory of NAFLD pathogenesis, lipid accumulation initiates simple hepatic steatosis and subsequently triggers multiple insults, ultimately inducing non-alcoholic steatohepatitis (NASH). Zhang et al. (2015) reported that up-regulation of miR-125b by estrogen protected against NAFLD in female mice. Hepatic miR-33a/miR-144 and their target gene ABCA1 were associated with steatohepatitis in morbidly obese subjects (Vega-Badillo et al., 2016), and down-regulation of miR-144 elicited proinflammatory cytokine production by targeting toll-like receptor 2 in nonalcoholic steatohepatitis of high-fat-diet-induced metabolic syndrome E3 rats (Li et al., 2015). Based on our findings of increased BMI and VI with obesity resulting from DKA exposure, we posit that miR-144 and miR-125b possibly regulate lipid metabolism, and further induce lipid-metabolism-disorder syndrome. This study aimed to examine the novel regulatory functions and pathways for the two miRNAs using zebrafish as a model organism. Further, we addressed whether or not obesity in parents can affect lipid metabolism in offspring and further increase the incidence of metabolic syndrome, which poses the pathological basis for juvenile T2D.

The primary objective of this study was to examine the relationship between DKA chronic exposure and zebrafish lipid metabolism disorder including liver function abnormalities. Based on our previous miRNA-seq analysis of zebrafish exposure to DKAs, we first screened the differentially expressed and high-abundance miR-125b and miR-144, and then explored their regulatory roles in lipid metabolism-related target genes. These two candidate miRNAs are highly conserved in humans, zebrafish and mice, but their regulatory functions are not yet confirmed in zebrafish. Similarly, the toxicological effects of abnormal expression induced by DKA exposure have not been investigated in zebrafish. Agonists and inhibitors of miR-125b and miR-144 were synthesized *in vitro* and micro-injected into F1-zebrafish to explore their effects on functional knockdown and overexpression of lipid metabolism and related target genes. Additionally, the accumulation of lipids and lipid content of zebrafish were investigated in detail using frozen oil-red-O staining, whole mount oil-red-O staining and related physiological and biochemical indices. The results of this study provide a theoretical basis for evaluating the ecological risk of DKAs in real-world aquatic environments and hold potential for application to gene therapy of drug-induced diseases.

2. Materials and methods

2.1. Ethics statement

With regard to all experimental protocols using zebrafish, we followed guidelines of the Institutional Animal Care and Use Committee (IACUC) at Wenzhou Medical University. All zebrafish surgery was performed on ice to minimize suffering.

2.2. Chemical reagents and exposure protocols

Six DKAs (ofloxacin, ciprofloxacin, enrofloxacin, doxycycline, chlortetracycline, oxytetracycline) were gratis supplied by Amresco (Solon, OH, USA); purities were > 99% except for chlortetracycline (95%). Chemical structures and molecular weights for the six DKAs are shown in Fig. S1. Adult wild type zebrafish (AB strain) were purchased from a local supplier and acclimated to the laboratory with a light/dark, 14 h/10 h cycle in a circulation system with dechlorinated tap water (pH 7.0–7.5) at a constant temperature (28 ± 0.5 °C) (Westerfield, 1995). Embryos at 6 hpf (6 h post fertilization) were exposed to control (no DKAs) and DKA treatment levels of 12.5 and 25 mg/L (12.5 mg/L DKA treatment corresponds to 4.04, 4.06, 4.52, 5.76, 5.79 and 6.28 μmol/L for chlortetracycline, doxycycline, oxytetracycline, ofloxacin, enrofloxacin and ciprofloxacin, respectively). The six DKA species were added in equal weight concentrations and equal volumes. The DKA-exposure solution was renewed daily to maintain stable exposure concentrations throughout the experimental period. Each treatment included 3 tanks, which represented 3 biological replicates. In total, 9 tanks (20 zebrafish in each tank) were used for 3 treatments (control and two DKA concentrations). Dechlorinated tap water (4 L) was added to a standard tank (27 cm length × 17.5 cm width × 21.5 cm height) for breeding F0-zebrafish. After DKA exposure to F0-zebrafish from 6 hpf to 90 dpf, F1-embryos were collected and not further exposed to DKAs prior to experimental trials.

2.3. Bioinformatics analyses

We used 5-dpf F1-zebrafish for miRNA sequencing and bioinformatics analyses. The miRNAs were screened for high abundance (per kilobase of exon per million fragments mapped (FPKM) ≥ 500) and positive differential expression (with $\log_2(|\text{fold-change}|) \geq 1$ and p-value < 0.05) using miRBase Targets Release Version 5 software (http://www.ebi.ac.uk/enright-srv/microcosm). TargetScan software (http://www.targetscan.org/MicroCosm) was applied for predicting potential target genes. A potential network between miRNAs and their target genes was constructed by Cytoscape software (v3.0.1).

2.4. Analyses of miRNAs and expression of their target genes using qRT-PCR

qRT-PCR was performed to investigate the effects of DKA exposure on the expressions of miRNAs and their related target genes regulating

lipid metabolism. We used the All-in-One TM miRNA qRT detection system (Genecopoeia, Rockville, USA), followed by SYBR Green PCR analysis (Bio-Rad, Hercules, USA), to confirm and measure the expression of miRNAs and their target genes regulating lipid metabolism. The forward primers for miRNAs were designed and synthesized by Sangon Biotech (Shanghai, China) and the reverse primers were the universal set provided by Genecopoeia with U6 as the endogenous reference. The forward and reverse primers for target genes were designed and synthesized by Sangon Biotech with elfa as the endogenous reference (Table S1). All PCR analyses were performed for three biological replicates (27 × 3 zebrafish) and each biological replicate included three technical replicates. Bio-Rad CFX Manager software was used to analyze qRT-PCR results. Relative changes in miRNAs and target gene expression were analyzed using the $2^{-\Delta\Delta CT}$ relative quantification method.

2.5. Whole-mount in situ hybridization (W-ISH)

W-ISH was performed to characterize the spatial expression of target genes in 5-dpf F1-zebrafish obtained from DKA-exposed F0-zebrafish (6 hpf to 90 dpf). Each experiment included 3 biological replicates (27 × 3 zebrafish) and each biological replicate included three technical replicates. Probe synthesis was carried out by *in vitro* transcription, and W-ISH was performed using the method detailed by Thisse and Thisse (2008). Expression changes and distribution of target genes were assessed and photographed using an optical microscope (DM2700M, Leica, Germany).

2.6. Oil red O (ORO) and H&E staining

To explore whether DKA exposure affected lipid accumulation, we examined 90-dpf F0-zebrafish liver and 5-dpf F1-larvae following ORO staining (27 × 3 F1-larvae) (Kudo et al., 2007; Yoganantharjah et al., 2017). Additionally, H&E staining of 90-dpf F0-zebrafish liver tissue was performed using paraffin-embedded tissue that was section-dried and stained using standard protocols (9 × 3 F0-zebrafish) (Li et al., 2016). Each experiment included 3 biological replicates and each biological replicate included three technical replicates. The tissue structure was observed by optical microscopy (Leica DM2700M, Heidelberg, Germany).

2.7. Lipid determination

Triglyceride (TG) and total cholesterol (TCH) kits were supplied by Ningbo Medical System Biotechnology (Ningbo, China). An Erba XL-640 analyzer (Berlin, Germany) was used to determine the lipid indexes of F0- and F1-zebrafish. Twenty-seven F0-zebrafish at 90-hpf for each group (control and two DKA treatments) were placed on ice to extract blood using a vacuum tube (9 × 3 F0-zebrafish). The serum was acquired by centrifugation for 15 min at 8000 rpm and 4 °C and subsequently stored at −80 °C until analysis. Twenty-seven F1-zebrafish larvae at 5-dpf for each group were collected and washed three times with phosphate-buffered saline (PBS). Each experiment included 3 biological replicates and each biological replicate included three technical replicates. According to F1-zebrafish weight, whole-mount larval tissue was diluted 10-fold using distilled water. The supernatant was acquired by centrifugation for 10 min at 8000 rpm and 4 °C and stored at −80 °C until analysis. TG and TCH were measured using enzymatic and colorimetric methods according to test kit instructions (Xie et al., 2016).

2.8. Microinjection

Agonists and inhibitors of miR-144 and miR-125b, along with negative sequences, were designed and synthesized *in vitro* by GenePharma (Shanghai, China). After dilution in 10 mM HEPES buffer (pH 7.6), they were microinjected into the one-to-four cell stage zebrafish embryos (200–400 pg/embryo; Pli-100A, Warner Instruments, Hamden, USA); any dead embryos were removed every 12 h. Twenty-seven embryos or larvae from each treatment were randomly selected and anesthetized with 0.03% tricaine methanesulfonate (buffered MS-222, Sigma, St. Louis, USA) for 30 s before observation using optical microscopy (Leica DM2700M).

2.9. RNA isolation and qRT-PCR after microinjection

qRT-PCR of miRNAs and their target genes was performed to validate the expression of miR-144 and miR-125b from zebrafish microinjected with agomir-144, agomir-125b, antagomir-144 and antagomir-125b. Total RNA from 5-dpf F1-zebrafish (27 × 3 larvae) was extracted using TRIzol reagent according to manufacturer's instructions (Invitrogen, Carlsbad, USA). Forward primers for the miRNAs were designed and synthesized by Sangon Biotech and the reverse primers were the universal set provided by Genecopoeia with U6 as the endogenous reference. The forward and reverse primers for target genes were designed and synthesized by Sangon Biotech with elfa as the endogenous reference (Table S1). We used the All-in-One™ miRNA and target gene qRT detection systems for miRNA (Genecopoeia) followed by SYBR Green PCR (Bio-Rad) analysis to confirm and measure the expression of miRNAs and their target genes after micro-injecting their agonists and inhibitors. Bio-Rad CFX Manager software was used to analyze the results from qRT-PCR. Relative changes in expression of miRNAs and their target genes were analyzed using the $2^{-\Delta\Delta CT}$ relative quantification method (Fu et al., 2006). All PCR reactions were performed using three biological replicates, and each biological replicate included three technical replicates. Finally, the average value for each group was considered for comparative analysis.

2.10. Effects of agonists and inhibitors

By means of the ORO staining method, the effects of agonists and inhibitors of miRNAs on lipid accumulation in zebrafish liver was investigated using micro-injection of agomir-144, agomir-125b, antagomir-144 and antagomir-125b. W-ISH was used to characterize the spatial expression of target genes in 5-dpf zebrafish after micro-injection of the four agomirs as detailed by Thisse and Thisse (2008).

2.11. Statistical analyses

Each experimental group (0, 12.5 and 25 mg/L DKAs) was composed of three biological replicates, and each biological replicate included three technical replicates to assess experimental accuracy and precision. All experimental data were reported as the mean ± SD (standard deviation). One-way analysis of variance (ANOVA) and Tukey's multiple comparison tests were applied to determine statistical differences between control and treatment groups. Statistical analyses were carried out using SPSS 19.0 (IBM, USA) at the $p < 0.05$ (*), $p < 0.01$(**) or $p < 0.001$(***) significance levels.

3. Results

3.1. Bioinformatics analyses

The miRNA sequencing and bioinformatics analyses for 5-dpf F1-zebrafish previously identified a high abundance of positive differentially expressed miRNA-144 and miRNA-125b for each DKA treatment based on the criteria of $Log_2(|\text{fold-change}|) \geq 1.0$, per million fragments mapped (FPKM) ≥ 100 and $p < 0.05$ (Zheng et al., 2016). To better understand the biological functions of miRNA-144 and miRNA-125b, we predicted their potential target genes using TargetScan software. According to the principles of lowest energy and highest score value in the TargetScan database, we screened out the specifically lipid

metabolism-related target genes of the two miRNAs by 3′-UTR binding information, and further analzyed the detailed information for these related target genes, which included pathway, chromosome location, binding site, binding area and context + score (Table S2). Fig. S2A shows a potential network between the two miRNAs, which were differentially expressed and possessed effective binding between 3′-UTR of the target gene and miRNA. A single miRNA concurrently regulates a large number of target genes, and *vice versa,* one gene may be regulated by multiple miRNAs (Fig. S2A). As a result, it constitutes a complex regulatory network between two miRNAs and their target genes.

Previous studies revealed that miRNAs tend to be clustered in introns or intergenic regions. The clustering patterns suggest that miRNAs in the same cluster might involve polycistronic transcription (Wang et al., 2016). The clustering of miRNA genomic locations is defined as two neighboring miRNAs located within 10 kb and on the same strand. BEDTools (Quinlan and Hall, 2010) was used to randomly shuffle the genomic locations of miR-125b and miR-144 loci to test whether the same cluster occurred in zebrafish and humans. We identified that miR-100 and let-7a were in the same clusters as miR-125b in zebrafish, and that miR-99a and let-7c were in the same clusters in humans. Additionally, miR-451 was identified as co-expressed in models with miR-144 in zebrafish and humans (Fig. S2C). As genes located in the same operon often have similar functions, miRNAs in the same cluster are ascribed to regulate functionally related genes.

The target pathways of miRNA-144 and miRNA-125b in humans and zebrafish as determined by DIANA miRPath V3 software (http://snf-515788.vm.okeanos.grnet.gr/) are shown in Figs. 1A and 1B, respectively. To date, there is a paucity of data regarding the target pathways of hsa-miR-125b and hsa-miR-451 in the same cluster as miR-144 in humans (Fig. 1A). The hsa-miR-144 is mainly associated with proteoglycans metabolism in cancer. The dre-miR-144 and dre-miR-125b primarily participate in pyrimidine and purine metabolism in zebrafish on the intersection pathway with dre-miR-451 and dre-let-7a (Fig. 1B). The target gene function of miR-125b was confirmed to be involved in fat metabolism in mice and human cells (Li et al., 2015). While few data are available concerning the common functions and metabolic pathways of miR-125b and miR-144 in zebrafish, the two miRNAs were highly conserved across the three vertebrate species (human, mice and zebrafish) (Fig. S2D).

A main goal of this study was to explore the regulatory functions of dre-miR-125b and dre-miR-144 in fat metabolism for the sake of enriching relevant databases. It is well known that the expression sites and distribution of miRNAs in different tissues and organs are strongly related to their functions. To further illustrate the functions of the two differentially expressed miRNAs, we analyzed the main expression sites of miR-125b and miR-144 in zebrafish and humans (http://www.microrna.org/microrna/getExprData.do; Wienholds et al., 2005; Landgraf et al., 2007). It was especially evident that the main expression system of miR-125b was observed in the central and peripheral nervous system, and that the main distribution was found in the brain, spinal cord, cranial and ganglia of zebrafish and humans. The miR-125b was also expressed in the cardiac and digestive systems of humans. In comparison, the main expression of miR-144 was in the cardiac system of zebrafish and humans, and in the central nervous system, respiratory system and gas system in humans. The distribution of miR-144 was in blood, erythroid cells and heart, as well as liver (Fig. S2B).

3.2. Expression levels of miRNA and their target genes after DKA exposure

Changes in miR-144 and miR-125b expressions, determined by qRT-PCR and using the U6 signal as a stable reference gene, were used to determine the effects of DKA exposure on 5-dpf F1-zebrafish. The 12.5 and 25 mg/L DKA-exposure treatments significantly increased the expressions of miR-144 and miR-125b at the $p < 0.001$ and $p < 0.01$ levels, respectively, as compared to the control (Fig. 2A). TargetScan databases indicated a high probability for target genes regulating lipid metabolism (*ppardb*, *bcl*2a, *pparaa* and *pparda*) based on low binding free energy to 3′-UTR of the target gene and high context + score. Expression levels of the four target genes were all significantly down-regulated ($p < 0.05$ or $p < 0.01$) in the 12.5 mg/L DKA treatment. In comparison, the 25 mg/L DKA treatment showed significantly decreased ($p < 0.01$ or $p < 0.001$) expression levels for *ppardb*, *bcl*2a and *pparaa* compared with control, but no change in expression for *pparda* (Fig. 2B). In total, expression levels for miRNAs exhibited an inverse trend compared to their target genes. These changes in expression for target genes might lead to disorders in fat synthesis and metabolism.

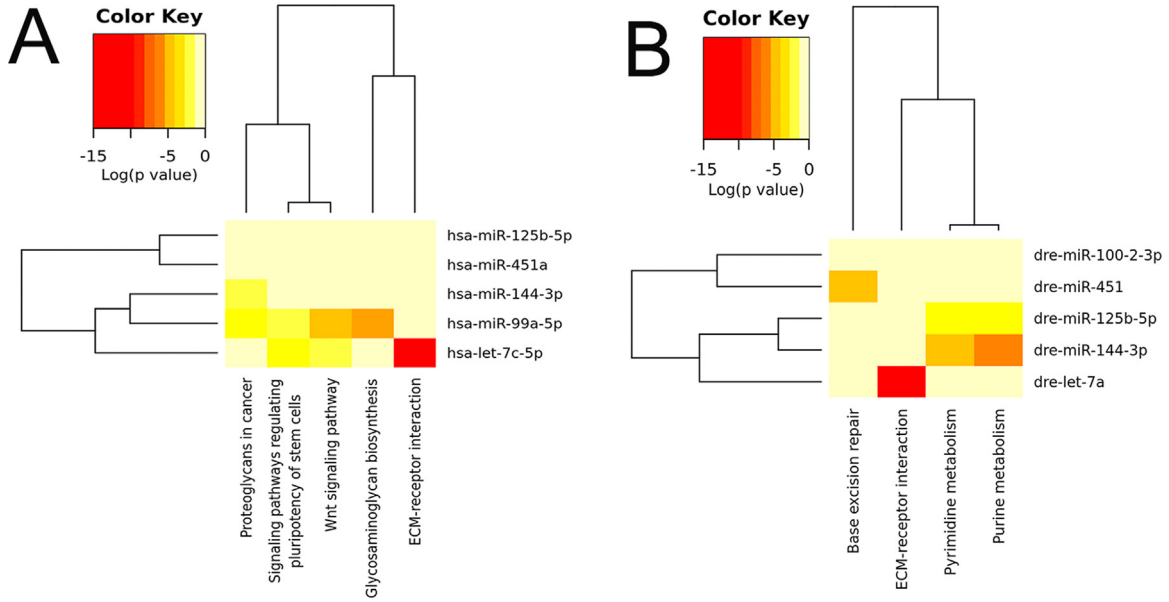

Fig. 1. Heat map and functional clustering patterns of miR-125b and miR-144 **Notes:** (1) A, heat map and functional clustering patterns of miR-125b and miR-144, and the same cluster of miRNAs in humans; (2) B, heat map and functional clustering patterns of miR-125b and miR-144, and the same cluster of miRNAs in zebrafish; (3) In heat map of miRNAs *vs.* pathways, miRNAs are clustered together by exhibiting similar pathway targeting patterns.

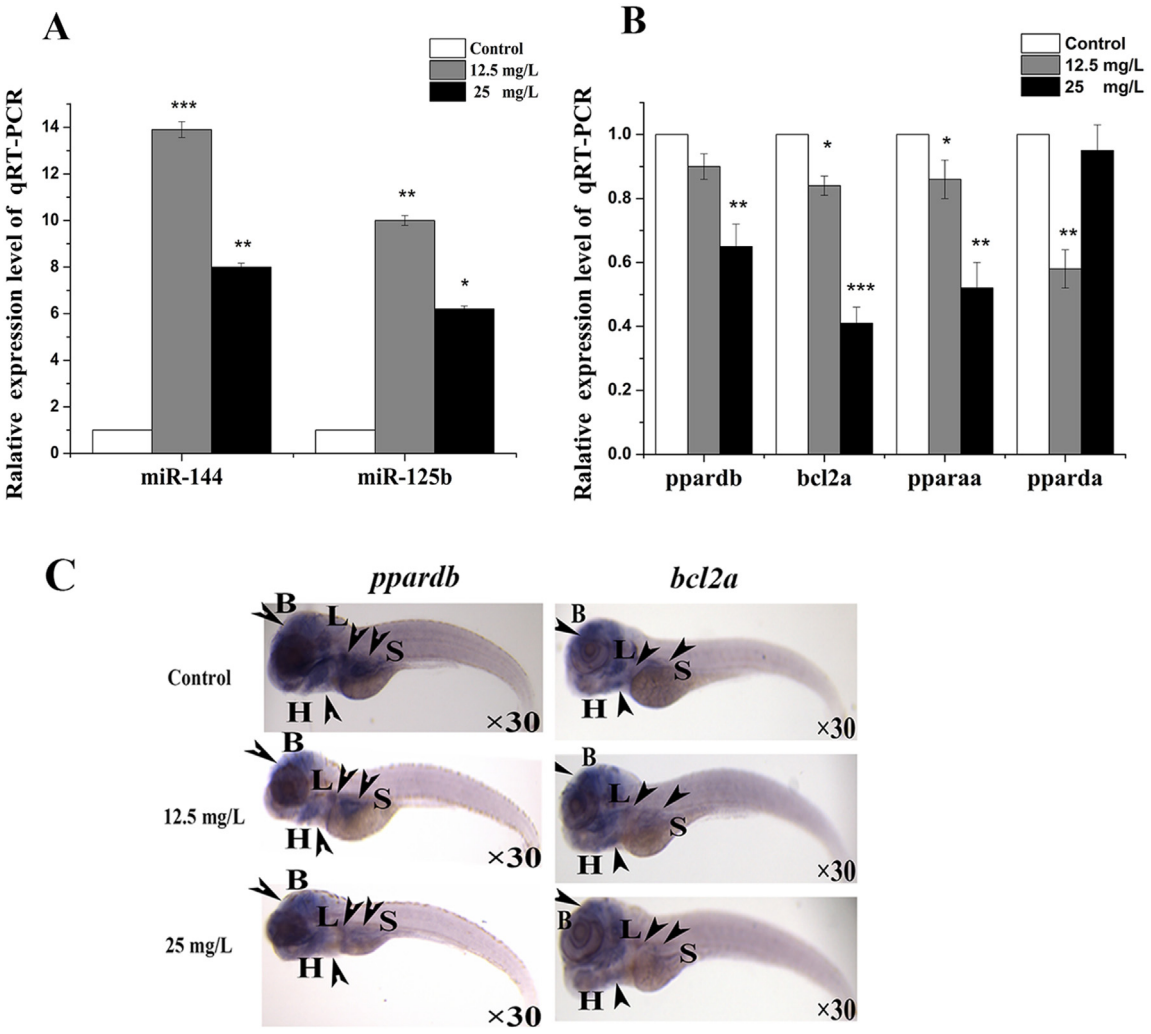

Fig. 2. Differential expressions of miR-125b and miR-144 and their target genes after DKA exposure by qRT-PCR, as well as W-ISH analysis of target gene expression
Notes: (1) A, relative fluorescence intensity units for miR-125b and miR-144; (2) B, qRT-PCR of target genes (*ppardb*, *bcl*2a, *pparaa*, *pparda*) of miR-125b and miR-144 after DKA exposure to 120-hpf larvae (n = 3, 27 larvae per group); (3) C, W-ISH of *ppardb* and *bcl2a* expression in 120-hpf larvae (n = 3, 27 larvae per group); (4) C, expression of hybridization signals for lateral, ventral and dorsal view in control and treatment groups; (5) Capital letters in Fig. 2C: B, brain; L, liver; S, swim bladder; H, heart; (6) Data are expressed as the mean ± SD; (7) *, ** and *** in Figs. 2A-2B indicate $p < 0.1$, $p < 0.05$ and $p < 0.01$, respectively, between DKA-exposure treatments and control; and (8) Dunnett's test statistical analysis.

3.3. Expression distribution and changes of target genes in F1-zebrafish by W-ISH

By means of W-ISH, the expression location, distribution and changing trend of *ppardb* and *bcl*2a in response to DKA exposure were identified in 5-dpf F1-zebrafish. The two target genes were mainly distributed in the brain, heart, liver and swim bladder (Fig. 2C). In the control group, both target genes showed high expression in the brain, heart, liver and swim bladder. In contrast, expression levels of *ppardb* and *bcl*2a were significantly decreased with increasing DKA-exposure concentrations ($p < 0.01$ or $p < 0.001$). Notably, the 25 mg/L DKA treatment showed a significant decrease in optical density compared with the control (Fig. 2C). Moreover, the expression pattern of *ppardb* and *bcl*2a by W-ISH was in general agreement with qRT-PCR results. These observations indicate that DKA exposure results in abnormal expressions of *ppardb* and *bcl*2a in the brain, heart, liver and swim bladder of F1-zebrafish resulting in disruption of lipid metabolism.

3.4. Whole-mount ORO staining analysis of F1-zebrafish

To further evaluate whether DKA exposure affected lipid metabolism in F1-zebrafish larvae, 5-dpf F1-zebrafish from F0-zebrafish exposed to DKAs (0, 12.5 and 25 mg/L DKAs) were stained using ORO. Whole-mount ORO staining showed that the brain and liver of 5-dpf F1-zebrafish larva had lipid droplet accumulation and the lipid droplets became more abundant and larger when F1-larva were from F0-zebrafish exposed to DKAs. The degree of lipid accumulation in the brain and liver showed a positive concentration-dependence (Fig. 3B). These histopathological phenomena demonstrated that chronic DKA exposure to zebrafish parents seriously affected lipid accumulation in F1-zebrafish and contributed to lipid-metabolism-disorder diseases, such as obesity, senility, nonalcoholic fatty liver disease and atherosclerosis.

3.5. Whole-mount ORO staining and H&E analysis of F0-zebrafish

To examine fatty liver of F0-zebrafish in response to DKA exposure, paraffin-coated liver sections stained with ORO and haematoxylin and eosin (H&E) were microscopically observed after a 90-day exposure to DKAs (0, 12.5 and 25 mg/L DKAs). Histopathological observations indicated that DKA exposure induced severe changes and damage to zebrafish liver tissue. Under 200× magnification, the liver structure in the control group was complete and clear, and the shape of hepatocytes

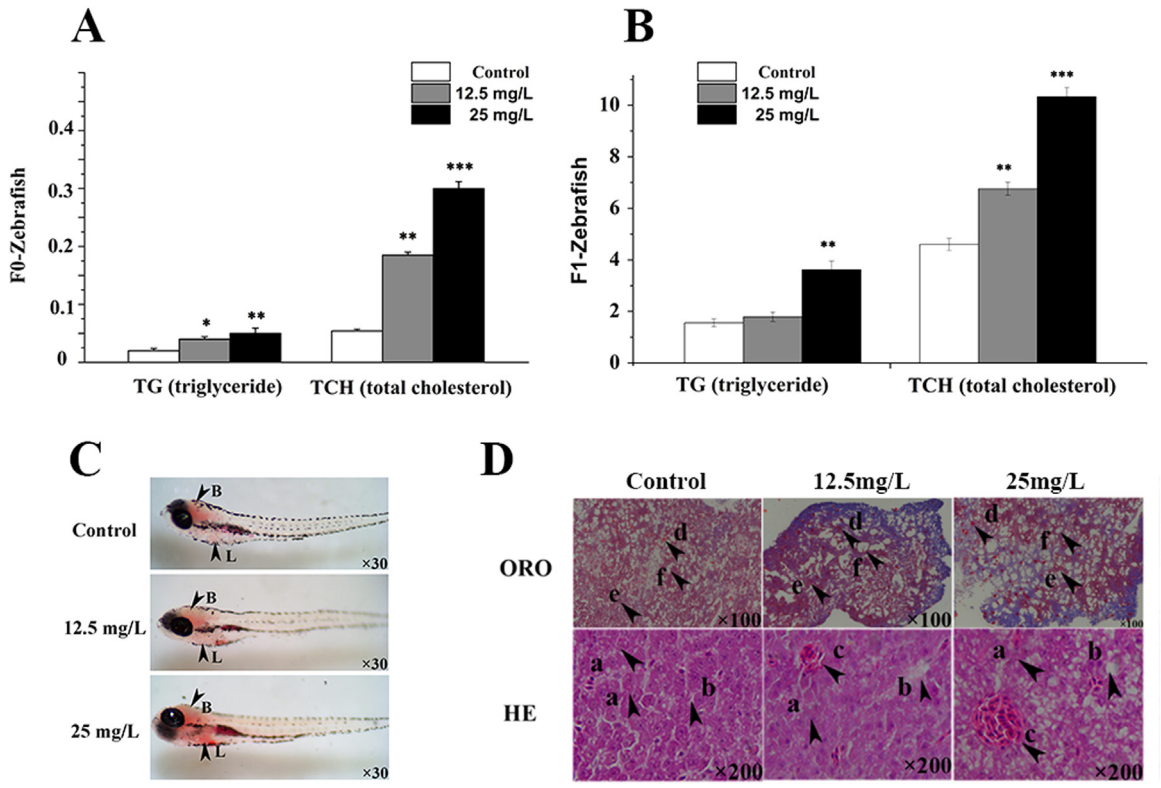

Fig. 3. ORO staining and TG and TCH levels in F0-zebrafish serum and F1-zebrafish larvae **Notes:** (1) A, TG and TCH levels in F0-zebrafish serum (n = 3, 27 zebrafish per group); (2) B, TG and TCH levels in F1-zebrafish larvae (n = 3, 27 zebrafish per group); (3) C, whole mount ORO staining of 5-dpf F1-zebrafish larvae (n = 3, 27 larvae per group); (4) D, histopathological ORO and HE staining of F0-zebrafish liver after 90 days of DKA exposure (0, 12.5 and 25 mg/L; n = 3, 9 zebrafish per group); (5) Capital letters in Fig. 3C: B, brain; L, liver; (6) Lowercase letters in Fig. 3D: a and b, blood accumulation; c, clot formation; d, lipid drops and the distribution area; e and f, fibrosis; (7) Data are expressed as the mean ± SD; (8) *, ** and *** in Fig. 3B indicate $p < 0.1$, $p < 0.05$ and $p < 0.01$, respectively, between DKA-exposure treatments and control; and (8) Dunnett's test statistical analysis.

was regular and arranged in tubules with uniform nucleus and clear configuration. In contrast, liver structure of the 12.5 mg/L DKA treatment displayed fibrosis, increased number of lipid droplets, a greater distribution area, wider cell gap, and a relatively scattered cell distribution. Further in the 25 mg/L DKA treatment, hepatic fibrosis became severe, the number and distribution area of lipid droplets were prominently increased, there was more irregular cell distribution with different cellular morphology, and hepatocytes displayed bubbles with severe fibrosis and fatty degeneration. Blood accumulation and clot formation were also noticed in the liver tissue (Fig. 3D). The degree of damage and lipid accumulation in the liver increased with increasing DKA-exposure concentrations (Fig. 3D). These histopathological phenomena demonstrate that chronic DKA exposure severely injures the liver of zebrafish and causes NFLD and fat metabolism disorder syndrome. Based on our previous study, chronic DKA exposure to adult zebrafish (6-hpf to 90 dpf) led to an increasing proportion of female to male zebrafish and a decreasing body mass index (BMI) in the 12.5 mg/L DKA treatment ($p < 0.05$) of female zebrafish (Li et al., 2016). These results indicate that obesity was possibly induced by exposure to high DKA concentrations.

3.6. Changes in triglyceride (TG) and total cholesterol (TCH) levels

We measured TG and TCH concentrations in F0-zebrafish serum and F1-zebrafish larvae as two key indices of blood lipid content. TG concentration in F0-zebrafish serum was significantly higher in the 12.5 mg/L ($p < 0.05$) and 25 mg/L ($p < 0.01$) DKA treatments than in the control group (Fig. 3A). In the F1-zebrafish larva, TG content was significantly higher in the 25 mg/L treatment ($p < 0.01$), but there was no difference in the 12.5 mg/L treatment compared to the control group. Similarly, TCH levels in F0-zebrafish serum and F1-zebrafish larvae increased with increasing DKA-exposure concentrations, showing a positive concentration-dependence. Notably in the 25 mg/L DKA treatment, the TCH content sharply increased by more than 5-fold compared with the control group (Fig. 3B). Consequently, these observations demonstrate that chronic DKA exposure severely altered the normal levels of TG and TCH in zebrafish resulting in increased risk of hyperlipidemia, atherosclerosis and coronary heart disease.

3.7. Expressions of miRNAs and their target genes after micro-injecting agonists and inhibitors

Over-expression of miR-144 and miR-12b was achieved by micro-injecting miR-144 agomir or miR-125b agomir into the one-to-four cell stage of zebrafish embryos; the agomir was a synthetic RNA oligonucleotide that mimicked the miR-144 or miR-125b precursor. In contrast, knockdown of miR-144 or miR-125b was achieved by micro-injecting miR-144 antagomir or miR-125b antagomir, which was a chemically modified antisense oligonucleotide designed to specifically target mature miR-144 and miR-125b. The efficient over-expression and knockdown of miR-144 and miR-125b in zebrafish larvae (5-dpi) are illustrated in Fig. 4A. The miR-144 levels increased by approximately 5-fold when micro-injecting miR-144 agomir at 200 μg/mL. However, miR-144 levels decreased to approximately 40% of normal levels when embryos were treated with the miR-144 antagomir. In comparison, miR-125b levels increased by approximately 3-fold when micro-injecting miR-125b agomir, and levels dropped to approximately 20% of normal levels when embryos were treated with the miR-125 antagomir. These results demonstrate the efficacy of agomir/antagomir micro-injection for artificial intervention of miR144 and miR-125b levels.

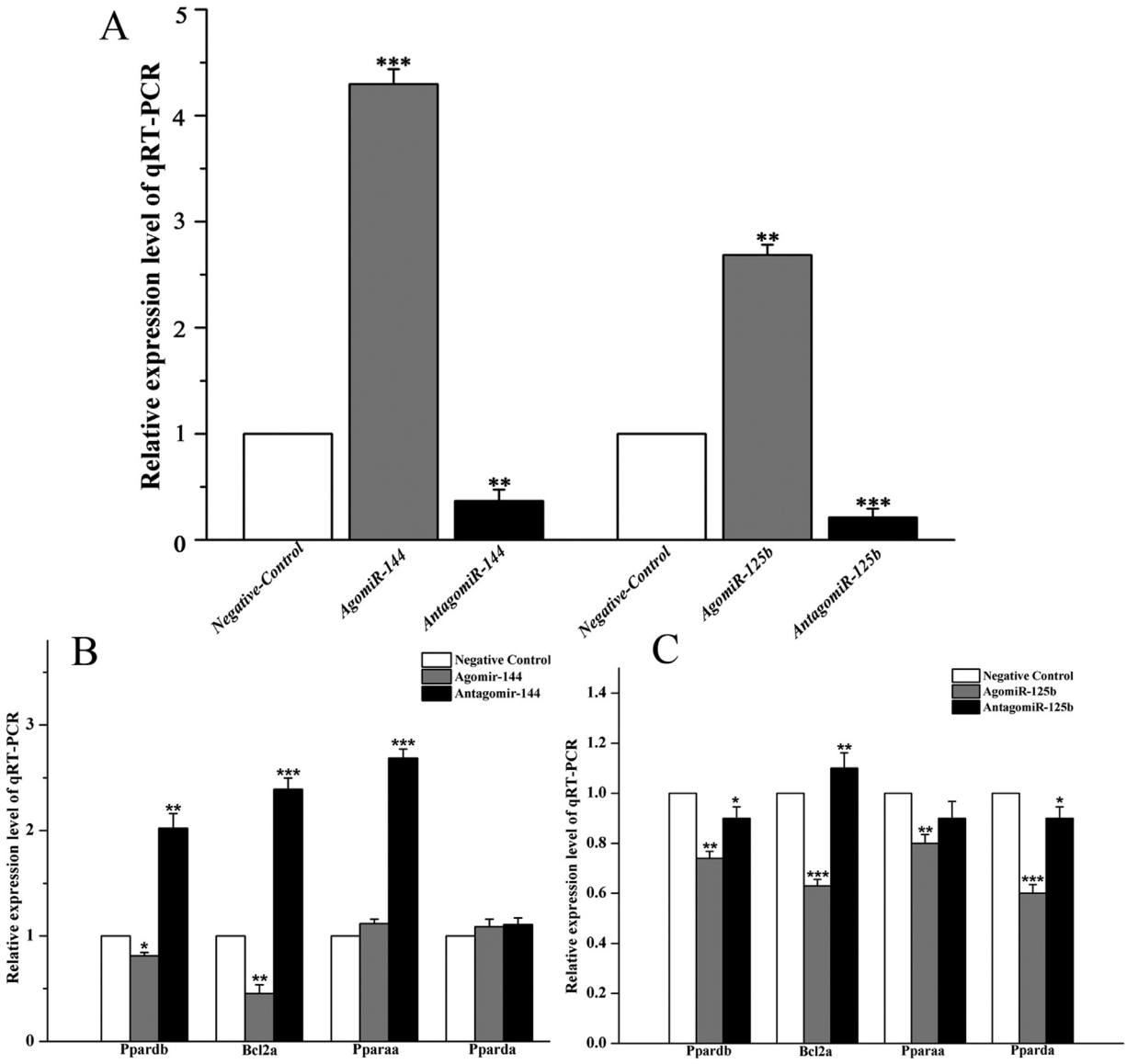

Fig. 4. Differential expression of miRNAs and their target genes after microinjection by qRT-PCR **Notes:** (1) A, qRT-PCR of miR-144, miR-125b expression after microinjection in 120-hpf larvae (n = 3, 27 larvae per group); (2) B, qRT-PCR of target genes after microinjecting miR-144 agonists and inhibitors in 120-hpf larvae (n = 3, 27 larvae per group); (3) C, qRT-PCR of target genes after microinjecting miR-125b agonists and inhibitors in 120-hpf larvae (n = 3, 27 larvae per group); (4) Data are expressed as the mean ± SD; (5) *, ** and *** in Figs. 4A-4C indicate $p < 0.1$, $p < 0.05$ and $p < 0.01$, respectively; and (6) Dunnett's test statistical analysis.

Moreover, the over-expression of lipid-metabolism related target genes (*ppardb*, *bcl*2a, *pparaa* and *pparda*) was achieved by micro-injecting miR-144 antagomir (Table 1). Levels of *ppardb* and *bcl2a* were successfully decreased in miR-144 agomir-microinjected zebrafish embryos (Fig. 4B). Similarly, micro-injecting miR-125b agomir to zebrafish embryos resulted in decreased levels of *ppardb*, *bcl2a*, *pparaa* and *pparda*. The levels of *bcl2a*, *ppardb*, *pparaa* and *pparda* were successfully up-regulated by micro-injecting miR-125b antagomir compared with the negative control and miR-125b agomir (Fig. 4C). Therefore, expression levels of miR-144 and miR-125b in zebrafish larvae can be effectively manipulated by regulating their target genes involved in lipid metabolism. Under DKA exposure, up-regulation of miR-125b and miR-144 inhibit the expression of fat-metabolism related genes.

3.8. W-ISH and ORO staining analysis of F1-zebrafish following manual intervention of miRs

To further illustrate the regulatory relationship between miRNAs and their target genes, we performed W-ISH to explicitly show the expression location, distribution and changes in expression levels for *ppardb* and *bcl*2a in F1-zebrafish after micro-injection of agomir-144, agomir-125b, antagomir-144 and antagomir-125b. The antisense oligonucleotide probes (848 and 786 bp) of *ppardb* and *bcl*2a were synthesized for W-ISH using *in vitro* transcription; the primers are listed in Table S1. The sequencing results demonstrate that the correct probes were synthesized for *ppardb* and *bcl*2a (Fig. S3). In the control group, the two target genes were mainly distributed and abundantly expressed in the brain, heart, liver and swim bladder of 5-dpf F1-zebrafish (Fig. 5A). Over-expression of the two target genes was achieved by micro-injecting miR-144 and miR-125b-antagomir, which resulted in increased optical density prominently in the brain, heart, liver and swim bladder. Conversely, the expression levels of *ppardb* and *bcl*2a were obviously decreased in miR-144 and miR-125b-agomir micro-injected zebrafish embryos. The changing trend in expression observed for *ppardb* and *bcl*2a by W-ISH was consistent with qRT-PCR results. Additionally, micro-injecting miRNA agomirs or antagomirs affected

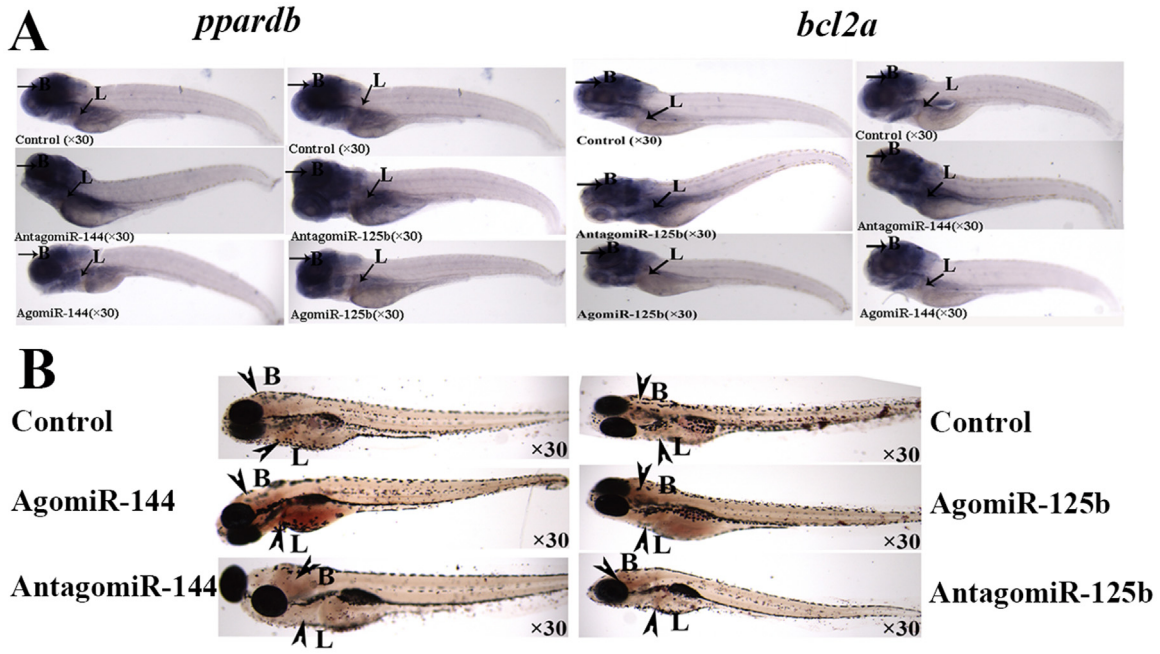

Fig. 5. W-ISH analysis of miR-144 and miR-125b expressions and their target genes, as well as ORO staining analysis after microinjection **Notes:** (1) A, W-ISH of *ppardb* and *bcl2a* expression after microinjecting miR-144 and miR-125b agonists and inhibitors, respectively (n = 3, 27 larvae per group); (2) B, whole mount ORO staining of F1-zebrafish larvae (5-dpf) after microinjecting miR-144 and miR-125b agonists and inhibitors, respectively (n = 3, 27 larvae per group); (3) A and B expression of hybridization signals for lateral view in control and treatment groups; and (4) Capital letters in Figs. 5A and 5B: B, brain; L, liver.

lipid accumulation in the brain and liver of larval zebrafish. The whole-mount ORO staining showed that the brain and liver of F1-zebrafish larvae (5-dpf) had lipid droplet accumulation and the droplets became more abundant when larvae were micro-injected with miR-144-agomir or miR-125b-agomir compared to the control group. In contrast, when miR-144-antagomir or miR-125b-antagomir were micro-injected into larvae, accumulation of lipid droplets in the liver and brain was significantly decreased compared to the control group. These phenomena demonstrate that over-expression of miR-144 and miR-125b consistently increased lipid accumulation in F1-zebrafish, which could further induce lipid-metabolism-disorder syndrome. These observations indicate that miR-144 and miR-125b can act as potential target molecules for hyperlipidemia drugs and as a reference for development of microRNA drugs.

4. Discussion

Our previous investigations examined the effects of DKAs on F0-zebrafish growth, development and behavior, and found that DKAs seriously disrupted liver development and resulted in increased BMI and VI for zebrafish from 4 hpf to 90 dpf (Li et al., 2016). Sequencing data showed that target genes regulated by high-abundance and positive differentially expressed miRNAs were involved in cancer, hepatitis B, cell cycle, Salmonella infection, metabolism of fatty acid synthesis, *etc.* (Zheng et al., 2016). However, these results were based on bioinformatics prediction from sequencing data and required further verification. As demonstrated from Figs. 1A-1B, there are few functional studies concerning miR-144 and miR-125b in humans and zebrafish. Based on our previous studies, we posited that chronic exposure to DKAs might lead to zebrafish lipid metabolism disorder and liver function abnormalities.

In this investigation, DKA-induced fat metabolism in zebrafish was demonstrated by several complementary techniques such as micro-injection intervention of agomir/antagomir, W-ISH, ORO staining and assessment of related physiological and biochemical indices. ORO staining is effective for rapid quantification of lipids in a variety of organisms and microorganisms (Yoganantharjah et al., 2017). Our previous studies using ORO staining reported changes in lipid content in the brain and yolk of zebrafish larvae after exposure to triclosan and its chlorinated derivatives (Zhang et al., 2018). Herein, we found that the degree of lipid accumulation in the larval brain and liver changed upon DKA exposure to parents using whole mount ORO staining. Frozen-section ORO staining indicated that DKA exposure affected the amount and size of lipid droplets in F0-zebrafish liver. Moreover, changes in TG and TCH levels also verified this phenomenon.

miRNAs have many physiological and pathological functions including a significant impact on lipid homeostasis (Norata et al., 2013; Thomou et al., 2017). In the present study, we reported two novel miRNAs, miR-144 and miR-125b, which regulated the expression of lipid-metabolism related genes (*ppardb*, *bcl2a*, *pparaa* and *pparda*) in the brain, heart, liver and swim bladder of F1-zebrafish, and further resulted in disruption of lipid metabolism. Peroxisome proliferator-activated receptors (PPARs) are enzymes that act as critical regulators of lipid oxidation and transport (Dharap et al., 2015; Poulsen et al., 2012). The miRNA-144 is a key miRNA in the pathological process of T2D, which is an important component of the insulin-signaling cascade that plays an important role in regulating insulin in muscles (Karolina et al., 2011). The prevalence of metabolically healthy obesity (MHO) over time and the incidence of type 2 diabetes mellitus (T2DM) in MHO were compared with metabolically healthy non-obesity (MHNO). This assessment demonstrated that obesity increased risk of dyslipidemia by 64% in metabolically healthy adults, however, obesity increased risk of diabetes by 240% in metabolically healthy adults (Fingeret et al., 2018). T2DM patients with obesity had higher fetuin-A levels as compared to non-obese patients and obese glucose tolerance (NGT) subjects ($p < 0.001$) (Zhou et al., 2018). The miR-144 was one of the highly up-regulated miRNAs that showed a linear increase in expression with increasing glycaemic status. In patients with T2DM, the expression level of miR-144 was significantly higher ($p < 0.01$) than normal subjects.

ABCA1, identified as a potential target of miR-144-3p, is a cell membrane protein mediating the transport of cholesterol, phospholipids and other metabolites from cells to lipid-depleted HDL apolipoproteins. miR-144-3p mimics (agomir) inhibit the expression of ABCA1 and enhance inflammatory factors. They also inhibit cholesterol efflux

in mice fed a high-fat diet (HFD), leading to accelerated pathological progression of atherosclerosis in experimental mice (Hu et al., 2014). The level of serum miR-144 was negatively related to serum high-density lipoprotein (HDL), but positively related to serum glucose levels. High serum glucose can lead to atherosclerosis and the majority of people with diabetes die from complications of atherosclerosis. Therefore, serum glucose levels may be an important early diagnostic biomarker for complications of atherosclerosis. Under chronic DKA exposure, miR-144 was predicted to regulate target genes related to the metabolism of glucose, lipid and carbohydrate, inducing obesity, and increasing risk of T2DM, hyperlipidemia and atherosclerosis.

The miR-125b and its close homolog miR-125a differ by a single nucleotide and are members of the miR-125 family of microRNAs. Both miR-125a and miR-125b can suppress endothelin-1 expression by directly targeting the 3-UTR region of preproET-1 mRNA. Decreased expressions of miR-125a and miR-125b are negatively associated with up-regulation of pre-proET-1 expression in the aorta of stroke-prone spontaneously hypertensive rats (SHR-SPs) (Li et al., 2010). Herrera et al. (2009) reported on the expression of 170 miRNAs in liver and adipose tissue of GK and BN rats and found the most significant expression change was for miR-125a in liver. The miR-125b can regulate cell proliferation, inhibit osteoblastic differentiation in mice mesenchymal stem cells and accelerate adipogenic differentiation *in vitro* (Mizuno et al., 2008). There is a reciprocal relationship between differentiation of osteogenesis into fat and inhibiting osteogenesis differentiation that in turn increases fat. Over-expression of miR-125b can suppress osteoblastic differentiation by multipotent mesenchymal stromal cells (MSCs) through directly modulating the target Smad4, a predicted target in silicon (Lu et al., 2013). Therefore, miR-125b plays an important role by inhibiting osteogenetic differentiation and promoting fat synthesis. The aforementioned results implied that miR-125b was related to the transformation of osteogenesis to fat. Li et al. (2015) reported that miR-125b expression was activated by estrogen *via* ERa *in vivo*. The miR-125b over-expressed adenoviruses were resistant to hepatic steatosis induced by a high-fat diet in ovariectomized or liver-specific ERa knockdown mice, due to decreased fatty acid uptake and synthesis and decreased triglyceride synthesis. Conversely, inhibiting the physiological role of miR-125b with a sponge decoy slightly promoted liver steatosis with a high-fat diet (Li et al., 2015), demonstrating that miR-125b could inhibit fat accumulation. These results from zebrafish are inconsistent with those in mice concerning changes in miR-125b and fat accumulation. Lin et al. (2017) demonstrated that triclosan induced an estrogen effect that acted on the novel estrogen receptor GPER leading to over-expression of miR-125b and further hepatic steatosis, while not on the classical ERα and ERβ. It is assumed that miR-125b influences fat-metabolism disorders through estrogen effects; however, the receptors identified in various reports are different (Li et al., 2015; Lin et al., 2017). Currently, NAFLD is the most common chronic liver disease worldwide and is a major public health concern in modern society (De Alwis and Day, 2008; Liu et al., 2017). Liver steatosis is a complex process modulated by many factors and its pathogenesis remains unclear. Therefore, molecular mechanisms involved in over-expression of miR-125b and fat accumulation due to DKA exposure are very complicated, but they provide important insights to better understand the molecular interactions involving lipid-metabolism disorders.

Acknowledgements

This work was jointly supported by the National Natural Science Foundation of China (31770552), and the Natural Science Foundation of Zhejiang Province (LY15C030004 and LY17H260004).

Appendix A. Supporting information

Supplementary data associated with this article can be found in the online version at doi:10.1016/j.ecoenv.2018.08.027.

References

Alavi, N., Babaei, A.A., Shirmardi, M., Naimabadi, A., Goudarzi, G., 2015. Assessment of oxytetracycline and tetracycline antibiotics in manure samples in different cities of Khuzestan province, Iran. Environ. Sci. Pollut. Res. 22, 17948–17954.
Chen, X., Ba, Y., Ma, L., Cai, X., Yin, Y., Wang, K., Guo, J., Zhang, Y., Chen, J., Guo, X., Li, Q., Zhang, C.Y., 2008. Characterization of microRNAs in serum: a novel class of biomarkers for diagnosis of cancer and other diseases. Cell Res. 18, 997–1006.
De Alwis, N.M., Day, C.P., 2008. Non-alcoholic fatty liver disease: the mist gradually clears. J. Hepatol. 48, 104–112.
Dharap, A., Pokrzywa, C., Murali, S., Kaimal, B., Vemuganti, R., 2015. Mutual induction of transcription factor PPARγ and microRNAs miR-145 and miR-329. J. Neurochem. 135, 139–146.
Fingeret, M., Marques-Vidal, P., Vollenweider, P., 2018. Incidence of type 2 diabetes, hypertension, and dyslipidemia in metabolically healthy obese and non-obese. Nutr. Metab. Cardiovasc. https://doi.org/10.1016/j.numecd.2018.06.011.
Fu, H.J., Zhu, J., Yang, M., Zhang, Y.Z., Tie, Y., Jiang, H., Sun, X.Z., Zheng, F.X., 2006. A novel method to monitor the expression of microRNAs. Mol. Biotechnol. 32, 197–204.
Herrera, B.M., Lockstone, H.E., Taylor, J.M., Wills, Q.F., Kaisaki, P.J., Barrett, A., Camps, C., Fernandez, C., Ragoussis, J., Gauguier, D., McCarthy, M.I., Lindgren, C.M., 2009. MicroRNA-125a is over-expressed in insulin target tissues in a spontaneous rat model of Type 2 Diabetes. BMC Med. Genom. 2, 54–58.
Hu, Y.W., Hu, Y.R., Zhao, J.Y., Li, S.F., Ma, X., Wu, S.G., Lu, J.B., Zheng, L., Wang, Q., 2014. An agomir of miR-144-3p accelerates plaque formation through impairing reverse cholesterol transport and promoting pro-inflammatory cytokine production. PLos One 9, 949–967.
Karolina, D.S., Armugam, A., Tavintharan, S., Wong, M.T., Lim, S.C., Sum, C.F., Jeyaseelan, K., 2011. MicroRNA-144 impairs insulin signaling by inhibiting the expression of insulin receptor substrate 1 in type 2 diabetes mellitus. PLos One 6, 228–239.
Krol, J., Loedige, I., Filipowicz, W., 2010. The widespread regulation of microRNA biogenesis, function and decay. Nat. Rev. Genet. 11, 597–610.
Kudo, T., Tamagawa, T., Kawashima, M., Mito, N., Shibata, S., 2007. Attenuating effect of clock mutation on triglyceride contents in the ICR mouse liver under a high-fat diet. J. Biol. Rhythms 22, 312–323.
Landgraf, J.M., 2007. Precision and sensitivity of the short-form pediatric enuresis module to assess quality of life (PEMQOL). J. Pediatr. Urol. 3, 109–117.
Li, D., Yang, P., Xiong, Q., Song, X., Yang, X., Liu, L., Yuan, W., Rui, Y.C., 2010. MicroRNA-125a/b-5p inhibits endothelin-1 expression in vascular endothelial cells. J. Hypertens. 28, 1646–1654.
Li, D., Wang, X., Lan, X., Li, Y., Liu, L., Yi, J., Li, J., Sun, Q., Wang, Y., Li, H., Zhong, N., Holmdahl, R., Lu, S., 2015. Down-regulation of miR-144 elicits proinflammatory cytokine production by targeting toll-like receptor 2 in nonalcoholic steatohepatitis of high-fat-diet-induced metabolic syndrome E3 rats. Mol. Cell Endocrinol. 402, 1–12.
Li, J.Y., Liu, J.F., Wang, X.D., Li, W.J., Zhang, H.Q., Wang, H.L., 2016. Screening on the differentially expressed miRNAs in zebrafish (*Danio rerio*) exposed to trace diketone antibiotics and their related functions. Aquat. Toxicol. 178, 27–38.
Li, L.L., Wang, Q.Y., Yuan, Z.Z., Chen, A.Q., Liu, Z.Y., 2018. LncRNA-MALAT1 promotes CPC proliferation and migration in hypoxia by up-regulation of JMJD6 via sponging miR-125. Biochem. Biophys. Res. Commun. 499, 711–718.
Lin, J., Wang, C., Liu, J., Dahlgren, R.A., Ai, W., Zeng, A., Wang, X., Wang, H., 2017. Upstream mechanisms for up-regulation of miR-125b from triclosan exposure to zebrafish (*Danio rerio*). Aquat. Toxicol. 193, 256–267.
Liu, X.L., Cao, H.X., Wang, B.C., Xin, F.Z., Zhang, R.N., Zhou, D., Yang, R.X., Zhao, Z.H., Pan, Q., Fan, J.G., 2017. miR-192-5p regulates lipid synthesis in non-alcoholic fatty liver disease through SCD-1. World J. Gastroenterol. 23, 8140–8151.
Lu, X., Deng, M., He, H., Zeng, D., Zhang, W., 2013. miR-125b regulates osteogenic differentiation of human bone marrow mesenchymal stem cells by targeting Smad4. Bull. Southeast. China Univ. 38, 341–346.
Lv, J., Kong, Y., Gao, Z., Liu, Y., Zhu, P., 2018. LncRNA TUG1 interacting with miR-144 contributes to proliferation, migration and tumorigenesis through activating the JAK2/STAT3 pathway in hepatocellular carcinoma. Int. J. Biochem. Cell Biol. https://doi.org/10.1016/j.biocel. 2018.05.010.
Mizuno, Y., Yagi, K., Tokuzawa, Y., Kanesaki-Yatsuka, Y., Suda, T., Katagiri, T., Fukuda, T., Maruyama, M., Okuda, A., Amemiya, T., Kondoh, Y., Tashiro, H., Okazaki, Y., 2008. miR-125b inhibits osteoblastic differentiation by down-regulation of cell proliferation. Biochem. Biophys. Res. Commun. 368, 267–272.
Mulgaonkar, A., Venitz, J., Sweet, D., 2012. Fluoroquinolone disposition: identification of the contribution of renal secretory and reabsorptive drug transporters. Expert Opin. Drug Met. 8, 553–559.
Ng, R., Wu, H., Xiao, H., Chen, X., Willenbring, H., Steer, C.J., 2014. Inhibition of mir-24 expression in liver prevents hepatic lipid accumulation and hyperlipidemia. Hepatology 60, 554–564.
Norata, G.D., Sala, F., Catapano, A.L., Fernándezhernando, C., 2013. MicroRNAs and lipoproteins: a connection beyond atherosclerosis? Atherosclerosis 227, 209–215.
Poulsen, L., Siersbæk, M., Mandrup, S., 2012. PPARs: fatty acid sensors controlling metabolism. Semin. Cell Dev. Biol. 23, 631–639.
Quinlan, A.R., Hall, I.M., 2010. BEDTools: a flexible suite of utilities for comparing genomic features. Bioinformatics 26, 841–842.
Shabani, N., Razaviyan, J., Paryan, M., Tavangar, S.M., Azizi, F., 2018. Evaluation of miRNAs expression in medullary thyroid carcinoma tissue samples: miR-34a and

miR-144 as promising overexpressed markers in MTC. Hum. Pathol. 8177, 30187–30194.
Song, L., Peng, L.P., Hua, S.C., Li, X.P., Ma, L.J., Jie, J., 2018. miR-144-5p enhances the radiosensitivity of non-small-cell lung cancer cells via targeting ATF2. Biomed. Res. Int. 5109497.
Thisse, C., Thisse, B., 2008. High-resolution in situ hybridization to whole-mount zebrafish embryos. Nat. Protoc. 3, 59–69.
Thomou, T., Mori, M.A., Dreyfuss, J.M., Konishi, M., Sakaguchi, M., Wolfrum, C., 2017. Adipose-derived circulating miRNAs regulate gene expression in other tissues. Nature 542, 450–455.
Tili, E., Michaille, J.J., Cimino, A., Costinean, S., Dumitru, C.D., Adair, B., 2007. Modulation of miR-155 and miR-125b levels following lipopolysaccharide/TNF-alpha stimulation and their possible roles in regulating the response to endotoxin shock. J. Immunol. 179, 5082–5089.
Vega-Badillo, J., Gutiérrez-Vidal, R., Hernández-Pére, H.A., Villamil-Ramírez, H., Hernández-Pando, R., Aguilar-Salinas, C.A., Canizales-Quinteros, S., 2016. Hepatic miR-33a/miR-144 and their target gene ABCA1 are associated with steatohepatitis in morbidly obese subjects. Liver Int. 36, 1383–1391.
Wang, Y.R., Luo, J.J., Zhang, H., Lu, J., 2016. microRNAs in the same clusters evolve to coordinately regulate functionally related genes. Mol. Biol. Evol. 33, 2232–2247.
Weber, J.A., Baxter, D.H., Zhang, S., Huang, D.Y., Huang, K.H., Lee, M.J., Galas, D.J., Wang, K., 2010. The microRNA spectrum in 12 body fluids. Clin. Chem. 56, 1733–1741.
Westerfield, M., 1995. The Zebrafish Book: A Guide For the Laboratory use of Zebrafish (*Danio rerio*). University of Oregon Press, Corvallis, USA, pp. 267–272.
Wienholds, E., Plasterk, R.H., 2005. MicroRNA function in animal development. FEBS Lett. 579, 5911–5922.
Xiao, F., Yu, J., Liu, B., Guo, Y., Li, K., Deng, J., 2014. A novel function of microRNA 130a–3p in hepatic insulin sensitivity and liver steatosis. Diabetes 63, 2631–2642.
Xie, X., Zhang, T., Zhao, S., Li, W., Ma, L., Ding, M., Liu, Y., 2016. Effects of n-3 polyunsaturated fatty acids high fat diet intervention on the synthesis of hepatic high-density lipoprotein cholesterol in obesity-insulin resistance rats. Lipids Health Dis. 15, 81–94.
Xu, L.Z., Li, T.F., Ding, W.D., Cao, Y., Ge, X.L., 2018. Combined seven miRNAs for early hepatocellular carcinoma detection with chronic low-dose exposure to microcystin-LR in mice. Sci. Total Environ. 628–629, 271–281.
Yin, H., Sun, Y.Q., Wang, X.F., Park, J.Y., Zhang, Y.Y., 2015. Progress on the relationship between miR-125 family and tumorigenesis. Exp. Cell Res. 339, 252–260.
Yoganantharjah, P., Byreddy, A.R., Fraher, D., Puri, M., Gibert, Y., 2017. Rapid quantification of neutral lipids and triglycerides during zebrafish embryogenesis. Int. J. Dev. Biol. 65, 105–111.
Zhang, Y.H., Liu, M., Liu, J.F., Wang, X.D., Wang, C., Ai, W.M., Chen, S., Wang, H.L., 2018. Combined toxicity of triclosan, 2,4-dichlorophenol and 2,4,6-trichlorophenol to zebrafish (*Danio rerio*). Environ. Toxicol. Pharmacol. 57, 9–18.
Zheng, Y.S., Lin, J.B., Li, J.Y., Zhang, H.F., Ai, W.M., Dahlgren, R.A., Wang, X.D., Wang, H.L., 2016. Effects of β-diketone antibiotics on F1-zebrafish (Danio rerio) based on high throughput miRNA sequencing under exposure to parents. Chemosphere 164, 41–51.
Zhang, Z.C., Liu, Y., Xiao, L.L., Li, S.F., Jiang, J.H., Zhao, Y., Qian, S.W., Tang, Q.Q., Li, X., 2015. Upregulation of miR-125b by estrogen protects against non-alcoholic fatty liver in female mice. J. Hepatol. 63, 1466–1475.
Zhou, Z.W., Ju, H.X., Sun, M.Z., Chen, H.M., Fu, Q.P., Jiang, D.M., 2018. Serum fetuin-A levels in obese and non-obese subjects with and without type 2 diabetes mellitus. Clin. Chim. Acta 476, 98–102.